ELSEVIER

Bioelectrochemistry 57 (2002) 23–32

Bioelectrochemistry

www.elsevier.com/locate/bioelechem

On the formation kinetics of two-dimensional cytidine films

Stanislav Hasoň [a,b], Vladimír Vetterl [a,b,*]

[a] Department of Physical Electronics, Laboratory of Biophysics, Faculty of Science, Masaryk University, Kotlářská 2, CZ-611 37 Brno, Czech Republic
[b] Institute of Biophysics, Academy of Sciences of the Czech Republic, Královopolská 135, CZ-612 65 Brno, Czech Republic

Received 23 February 2001; received in revised form 31 October 2001; accepted 5 November 2001

Abstract

The kinetics of phase transitions of cytidine adsorbed on mercury are studied by chronoamperometry and capacitance measurements. Cytidine forms highly ordered two-dimensional adlayers in a broad range of pH. In acid solvent, only one kind of condensed layer is formed. In the alkaline solution, cytidine forms two different two-dimensional (2D) adlayers. The minimum capacitance value in adlayer II at pH 5 is 7.0 μF cm^{-2} and, at pH 8.3, it is 5.1 μF cm^{-2}; in adlayer III, the minimum capacitance is 10.6 μF cm^{-2}. The formation of a physisorbed film of cytidine molecules adsorbed at the mercury surface proceeds by complex mechanisms. From $j-t$ transients, it can be seen that the phase transformations from dilute adlayer Ia to condensed physisorbed film II is accompanied by the reorientation of cytidine molecules at the mercury surface (inverted current transient). The interfacial transformations of the cytidine film yield a sigmoidal $C-t$ transient. This experimentally measured $C-t$ transient were analysed by Avrami theorem. The rate of the transformations from dilute adlayer Ia to condensed film II of cytidine at pH 5 depends strongly on temperature but is only slightly affected by temperature at pH 8.3. The effect of pH and ionic composition of the supporting electrolyte on the rate of transformation of cytidine films was studied as well.

Keywords: Two-dimensional phase transition; Adsorption; Nucleation and growth; Cytidine adlayers

1. Introduction

The studies of biologically important molecules at electrode/electrolyte interfaces as model systems are expected to provide valuable information on their behaviour at biological surfaces [1]. Such information will also be useful for the development of biosensors [2,3]. In the present paper, we are studying the effect of pH, temperature and ionic composition of solution on the adsorption and 2D condensation of cytidine at Hg electrode. The reason why we have chosen this nucleoside is that in the literature, there is less quantitative information on its adsorption and on the kinetics of film formation/dissolution [4–11] in comparison with the other nucleosides or DNA bases [12–24]. The present work is focused on a description of the kinetics of the formation of a physisorbed condensed cytidine film. We have fitted the kinetics data by Avrami theorem based on the nucleation and growth process.

* Corresponding author. Institute of Biophysics, Academy of Sciences of the Czech Republic, Královopolská 135, CZ-612 65 Brno, Czech Republic. Tel.: +42-5-4151-7143; fax: +42-5-4121-1293.

E-mail addresses: hason@physics.muni.cz (S. Hasoň), vetterl@ibp.cz (V. Vetterl).

2. Experimental

The electrochemical set-up consisted of a classical three-electrode system. The working electrode was a mercury drop electrode Metrohm 663 VA Stand (Zurich, Switzerland), operating as a hanging mercury drop electrode (HMDE). The drop area $A = 0.005$ cm^2 was determined by analysis of the cyclic voltammogram of reversible reaction of Cd^{2+} [25].

All potentials were measured with reference to an Ag/AgCl/3 M KCl electrode. Platinum wire was used as an auxiliary electrode.

The measurements were performed in a solution of NaCl (Merck, p.a.) and Britton–Robinson (BR) buffer. The pH value of this solution was adjusted by the addition of small amounts of concentrated HCl and/or NaOH. The BR buffer was prepared according to the literature [26] for each measured pH value. The ionic strength I of this solution was $I = 0.5$ mol kg^{-1}. Cytidine (Sigma) was used without any purification. The solutions were deaerated using 99.5% argon saturated with triple distilled water. The temperature was controlled with a cryostat at an accuracy of ± 0.1 °C.

All measurements were performed using an AUTOLAB electrochemical system (Ecochemie, Utrecht, Netherlands) equipped with a potentiostat/galvanostat PGStat20 and a

1567-5394/02/$ - see front matter
PII: S1567-5394(01)00179-7

frequency-response analyser (FRA) module. The differential capacitance of the electrode double layer and $C-t$ transients were measured using the FRA module at the following settings: frequency 33 Hz, AC voltage amplitude 5 mV, integration time 2 s, minimum number of cycles to integrate 5, number of cycles to reach steady state 10 and maximum time to reach steady state 3, with minimum fraction of a cycle 0. The CV measurement and $I-t$ transients were done using the AUTOLAB/GPES software.

3. Results and discussion

3.1. Effect of pH on the adsorption of cytidine in 0.5 M NaCl+BR buffer solution

Fig. 1 shows a typical cyclic voltammogram and the capacitance vs. potential curves ($C-E$ curves) of 30 mM cytidine in 0.5 M NaCl with BR buffer at two different pH values. Similar result was published and discussed earlier by Temerk et al. [5–7,10] and Ibrahim [11]. Cytidine is adsorbed at mercury in a wide potential range and different interfacial states can be distinguished, labelled Ia, Ib, II and III.

In acidic solution, the 2D condensation of adsorbed cytidine molecules and formation of a physisorbed compact layer takes place only in one potential region (region II), which is characterised by appearance of the capacitance pit on $C-E$ curve [4,12,27–29] and sharp current spikes on cyclic voltammograms at the potentials of the capacitance pit edges. The current spikes on the voltammograms (Fig. 1A, peaks A, A′ , B and B′) and the pit edges on the $C-E$ curves show hysteresis, i.e. their potential depends on the direction of the potential scan. Both the appearance of the capacitance pit and the hysteresis are typical properties of 2D physisorbed condensed films [1,30–33]. The differential capacitance in region II is 7.0 μF cm^{-2}. Region Ia and Ib corresponds to the dilute [1] reversible physical adsorption of individual cytidine molecules. At more negative potentials, cytidine is desorbed from the Hg surface ($E < -1.3$ V).

In alkaline solution, cytidine forms two different 2D physisorbed condensed layers. The centre of the first of them (region II) is located around −0.8 V (region II is delimited by the current spikes A, A′ , B and B′ , Fig. 1C). The second 2D physisorbed film is formed at more positive potentials. Region III is delimited by a pair of current peaks P and P′ . The differential capacitance value is 5.1 μF cm^{-2} in region II and 10.6 μF cm^{-2} in region III, i.e. about twice higher than in region II. This could mean that the cytidine layer thickness in region III is half of that in region II, and that cytidine is condensed there in planar orientation contrary to perpendicular orientation in region II. Another explanation for the higher capacitance in region III could

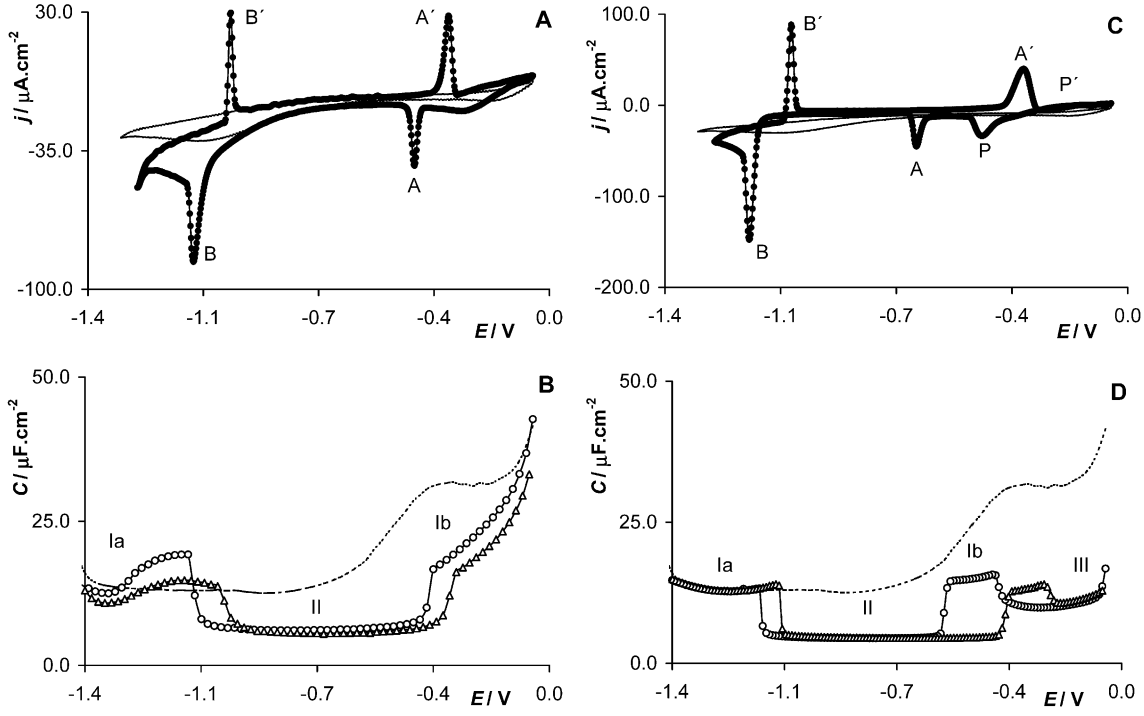

Fig. 1. Cyclic voltammograms of 0.5 M NaCl with BR buffer in the absence (solid line) and presence (●) of 30 mM cytidine at (A) pH 5 and (C) pH 8.3 at 10 °C. Capacitance–potential curves of 30 mM cytidine in 0.5 M NaCl with BR buffer at (B) pH 5 and (D) pH 8.3 at 10 °C. (○) Potential scan from −0.05 V to more negative potentials; (△) potential scan from −1.4 V to more positive potentials. Dashed line is background electrolyte. Conditions of measurements: (A,C) scan rate 100 mV s^{-1}, (B,D) frequency 33 Hz, AC voltage amplitude 5 mV, integration time 2 s, minimum number of cycles to integrate 5, number of cycles to reach steady state 10, maximum time to reach steady state 3. The different adsorption states are labelled as Ia, Ib, II and III.

be incorporation of the solvent anions into the condensed layer. In acid solutions, region III is not observed, probably because the protonated cytidine molecules, unlike the neutral ones, are repulsed from the positively charged mercury surface.

It was observed that the extent of region III is only slightly affected by a change of temperature (not shown). On the other hand, the capacitance pit width (region II) decreases with increasing temperature both in acid and alkaline solutions as it is usually observed [4,30,31,33]. The driving forces stabilising the 2D condensed film of cytidine in region II seems to be stacking interactions between cytosine rings perpendicularly oriented to the mercury surface [1,8,34]. From the temperature independence of the width of region III, it can be assumed that at neutral and alkaline pH, cytidine is chemisorbed on HMDE via the lone electron pair of N3. In acid solution, cytidine does not form a condensed layer in region III because cytidine is protonated at N3 and the chemical bond between mercury and cytidine cannot be formed. A similar behaviour was observed with chemisorbed surface films of uracil [35–38], uridine [39–41] and cytosine [42,43] at Au (111).

3.2. C–E–t measurements

In order to examine the establishment of the adsorption equilibrium in region II, we have measured $C-t$ curves. Figs. 2 and 3 show the $C-E-t$ surfaces [44–46] of 30 mM cytidine at potentials around the positive or negative edges of the capacitance pit (region II) in acidic (Fig. 2A,B) and alkaline pH (Fig. 3A,B). It can be seen that the effect of time on the capacitance pit (region II) is more complicated in alkaline pH (Fig. 3). In acid solution, a positive edge of the capacitance pit (region II) has a complex development contrary to the negative edge (Fig. 2B). The $C-E$ curves reconstructed from the isochronous $C-t$ plots [47,48] show that only at a very long time period ($t > 200$ s) the equilibrium state was reached (not shown). The $C-E-t$ surfaces of 30 mM cytidine around the potentials of the negative edge of the capacitance pit (region II) in alkaline (pH 8.3) and neutral (pH 7.2) solutions looks very similar (not shown).

The minimum capacitance value C_{min} of the cytidine adlayer in region II depends on pH. At pH 5, $C_{min} = 7.0$ μF cm^{-2} and, at pH 8.3, $C_{min} = 5.1$ μF cm^{-2}. In order to explain why the capacitance of the condensed cytidine layer depends on pH, we have studied the kinetic of the formation of this layer at both pH values.

3.3. Cyclic voltammograms of cytidine at different scan rates

Some information about the kinetics of cytidine adlayers can be obtained from the dependence of the peak potentials E_{max} and current maxima I_{max} of cyclic voltammogramms on the scan rate v_{scan}.

From Fig. 4, it can be seen that, at pH 5, the potential E_{max} of the peaks A, A′, B and B′ is independent on the scan rate. There is a linear dependence of the current maxima I_{max} on the square root of scan rate v_{scan} for all four peaks. Bosco and Rangarajan [49] have shown that this behaviour is characteristic for an instantaneous nucleation and growth process.

At pH 8.3 (Fig. 5), the peak potential E_{max} is slightly dependent on the scan rate. The dependence of the current maximum I_{max} (peak B′) on the scan rate has, at pH 8.3, a

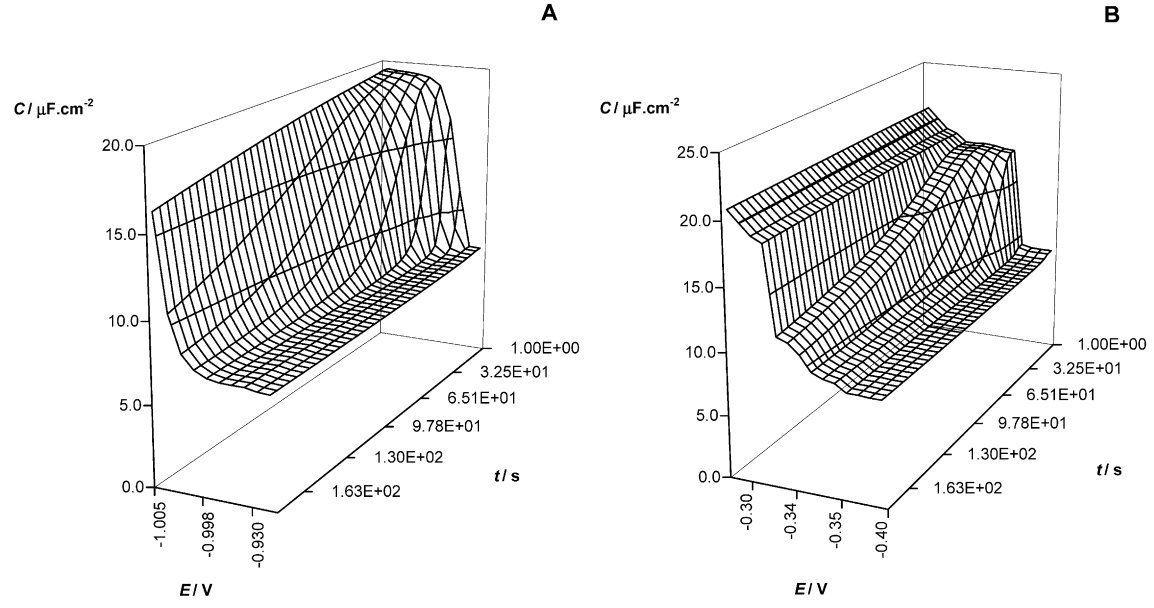

Fig. 2. $C-E-t$ surfaces of 30 mM cytidine in 0.5 M NaCl + BR buffer at potentials around the positive (A) or negative (B) edges of the capacitance pit (region II) in pH 5.

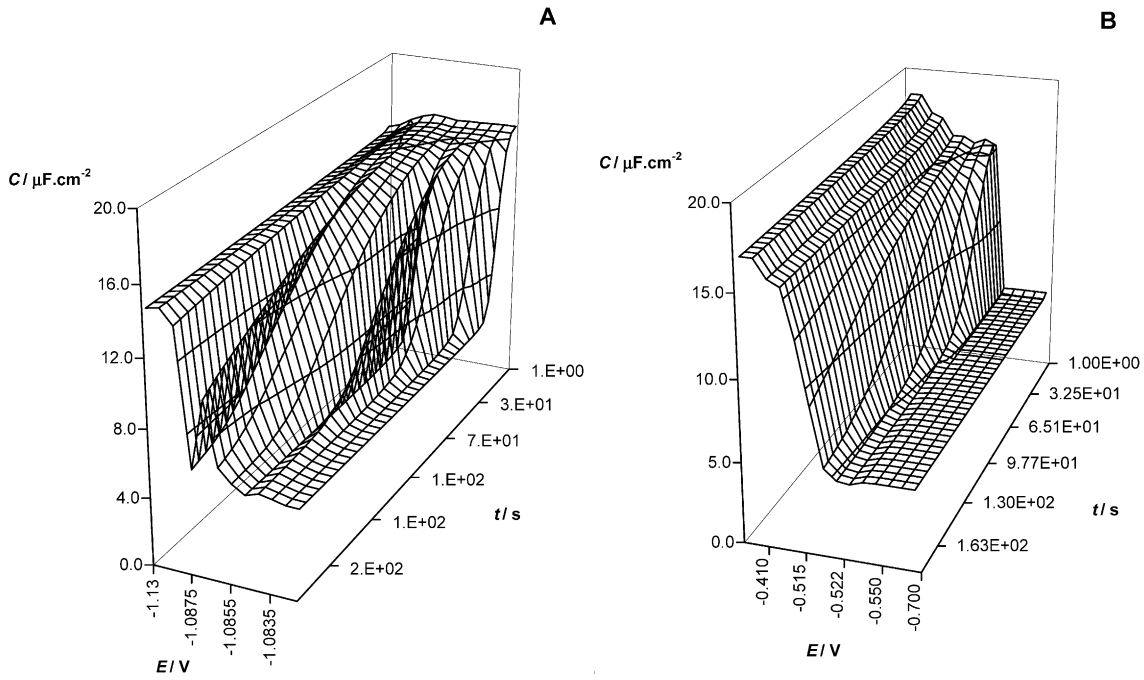

Fig. 3. $C–E–t$ surfaces of 30 mM cytidine in 0.5 M NaCl + BR buffer at potentials around the positive (A) or negative (B) edges of the capacitance pit (region II) in pH 8.3.

nonlinear course. Such behaviour is assumed for the progressive nucleation.

3.4. Kinetics of transformation

The formation of a self-assembled monolayer can be triggered at the electrochemical interface by an appropriate change in concentration, temperature or potential. The phase transformation is, however, usually initiated by applying a potential step, which may very rapidly trigger the formation of a new thermodynamically stable phase.

The kinetics of phase transformations of the cytidine on the mercury electrode were investigated by means of current and capacitance transients using the single potential step

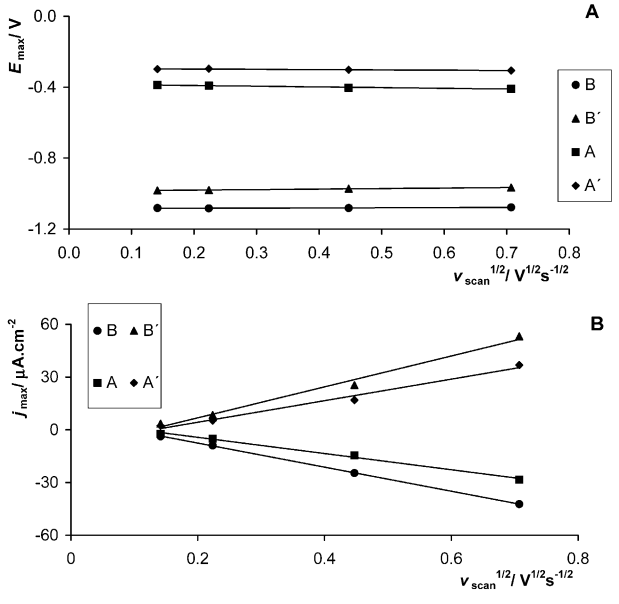

Fig. 4. Potentials E_{max} and current density maxima j_{max} of cyclic voltammogram peaks A, A′, B and B′ of 30 mM cytidine in 0.5 M NaCl + BR buffer at pH 5 as a function of the square root of scan rate v_{scan}.

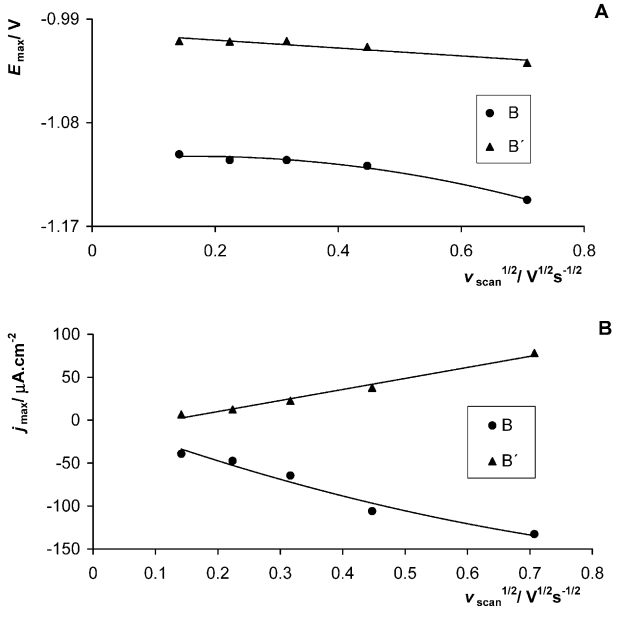

Fig. 5. Potentials E_{max} and current density maxima j_{max} of cyclic voltammogram peaks B and B′ of 30 mM cytidine in 0.5 M NaCl + BR buffer at pH 8.3 as a function of the square root of scan rate v_{scan}.

technique [32,33,50]. In order to minimise the time constant of the electrochemical cell, the concentration of the supporting electrolyte was sufficiently high (0.5 M).

The $C-t$ and $j-t$ transients were obtained after a single potential step from the initial potential E_i in the region of dilute adsorption Ia or Ib (waiting time at the potential E_i was $t=5$ s) to various final potentials E_f in the region II. The further is the final potential from the true thermodynamic transition potential E_T (potential of the pit edges of the equilibrium $C-E$ curves [14,45,50]), the shorter is the phase transition. With our instrumentation, it was not possible to find such a potential window in which the rate of the transition would allow to measure both $j-t$ and $C-t$ curves. (It was possible to measure $C-t$ curves only at times longer than 1 s).

The current transients encountered in polynucleation and growth processes on the mercury are commonly characterised by an exponential decay followed by a pronounced maximum, until finally, the current decreases to zero [23,24,50–52]. The current reaches its maximum at the time t_{max}, which is shorter at larger $|E_f-E_T|$ (overpotential) values.

The initial exponential decay is the sum of the double-layer charging due to the potential step itself and the Langmuir type (dilute) adsorption before the nucleation starts [53–55]. The current maximum is generally associated with a nucleation and growth process [35,56–60].

The mean current density reflects the changes in the surface charge due to the adsorption and condensation of the adsorbed molecules, i.e. the current flowing due to the charging of the growing condensed film (this current depends on $d\Theta/dt$) and the current flowing due to the changes in the surface concentration of the expanded dilute adsorption phase (depends on $d\Gamma/dt$) at the parts of the electrode surface not covered by the condensed film. The molecules adsorbed in the dilute layer are later incorporated in the growing condensed phase. If during condensation of adsorbed molecules their orientation and electronic properties are changed, an additional current occurs at the moment of condensation, a reorientation current, caused by the different dielectric properties of the dilute and condensed phases [61].

Depending on the value of the final potential E_f and on the direction of the permanent dipole moment of the adsorbed molecules, this reorientation current might have an opposite sign than the adsorption current and the oscillating current transients might be observed [52]; the current changes the sign during the transition. After the potential jump, the current decreases, crosses the zero charge line and becomes negative. Subsequently, the current increases, becomes positive and, after reaching maximum, decreases [52].

The first negative current part in the signal response is caused by a rapid condensation accompanied by an increasing depletion of the noncondensed phase around the growing islands of the condensed phase. With progressive

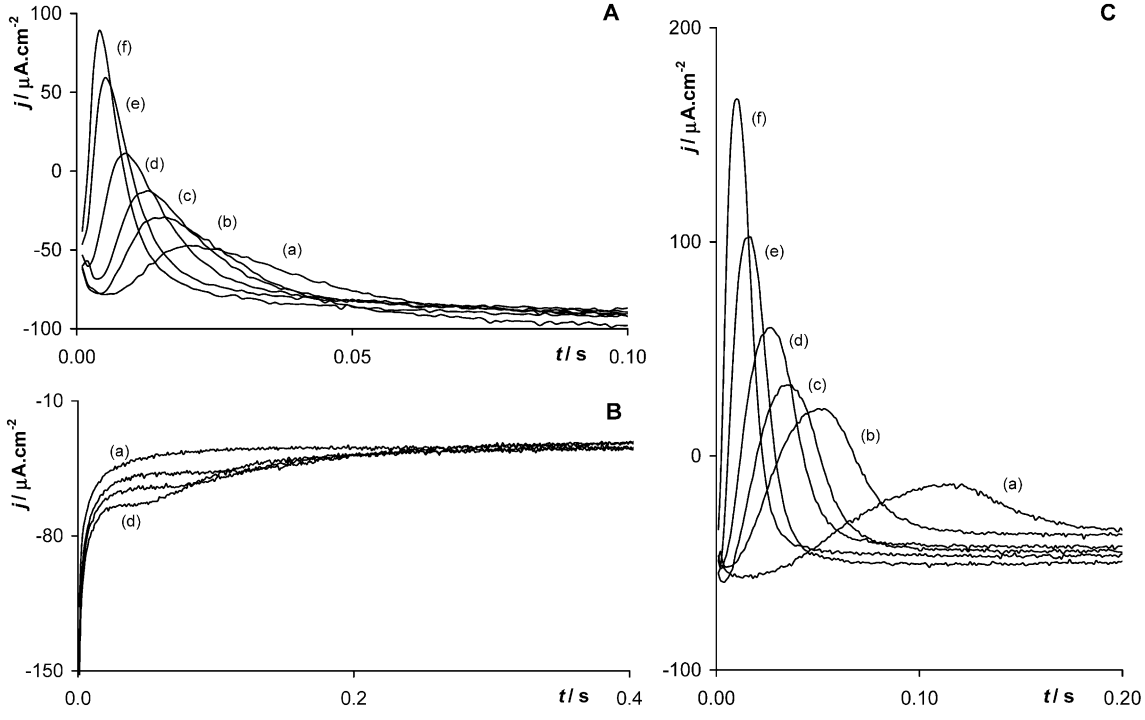

Fig. 6. (A) Current transients of 30 mM cytidine in 0.5 M NaCl + BR buffer at pH 5 triggered by a potential step from − 1.2 V (region Ia) to various final potentials close to the potential of peak B′ in Fig. 1A: (a) − 0.97, (b) − 0.965, (c) − 0.960, (d) − 0.955, (e) − 0.945 and (f) − 0.94 V. (B) Current transients triggered by a potential step from − 0.2 V (region Ib) to various final potentials close to the potential of peak A in Fig. 1A: (a) − 0.37, (b) − 0.38, (c) − 0.385 and (d) − 0.39 V. (C) Current transients of 30 mM cytidine in 0.5 M NaCl + BR buffer at pH 8.3 triggered by a potential step from − 1.2 V (region Ia) to various final potentials close to the potential of peak B′ in Fig. 1C: (a) − 1.04, (b) − 1.03, (c) − 1.025, (d) − 1.02, (e) − 1.01 and (f) − 1.0 V. The waiting time for the initial potentials was 5 s.

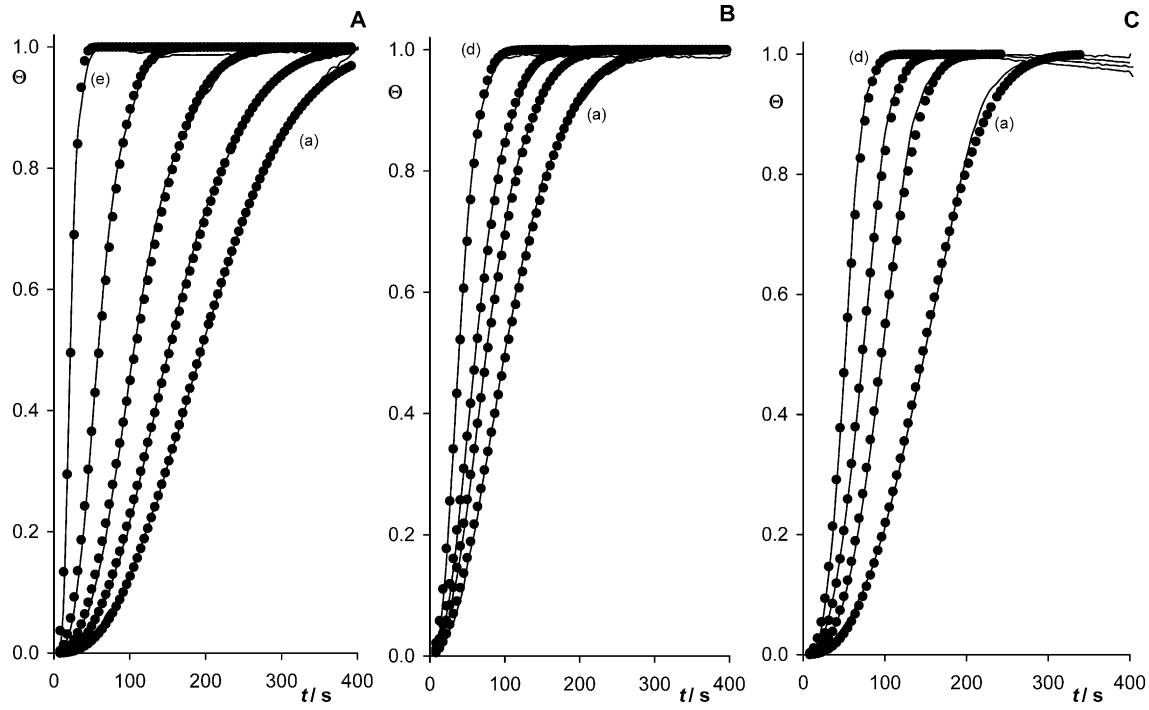

Fig. 7. (A) Dependence of the coverage degree Θ on time t for 30 mM cytidine in 0.5 M NaCl + BR buffer at pH 5 after a single potential step from − 1.2 V to various final potentials close to the negative edge of region II: (a) − 1.029, (b) − 1.027, (c) − 1.025, (d) − 1.023 and (e) − 1.02 V. (B) The Θ–t curves following a single potential step from − 0.2 V to various E_f close to the positive edge of region II: (a) − 0.338, (b) − 0.3393, (c) − 0.3398 and (d) − 0.341 V. (C) The Θ–t curves for 30 mM cytidine in 0.5 M NaCl + BR buffer at pH 8.3 after a single potential step from − 1.2 V to various final potentials close to the negative edge of region II: (a) − 1.088, (b) − 1.084, (c) − 1.082 and (d) − 1.08 V. (●) Numerical fit of the Θ–t curves were calculated according to Eqs. (2) and (3). The parameters of Eqs. (2) and (3) are listed in Tables 1–3. The waiting time for the initial potentials was 5 s.

coverage of the surface by condensed phase, the condensation current decreases. The depletion of the dilute phase leads to an increasing adsorption rate. The total current response becomes positive again until the whole surface is covered by the condensed phase [52].

3.4.1. j–t curves

Fig. 6A shows j–t curves for cytidine at pH 5 obtained by the potential step from $E_i = -1.2$ V (region Ia) to a different E_f in region II; E_f is located close to the negative edge of the capacitance pit. These current transients are characterised by an initial current increase followed by the gradual decay of the current. The transients start at negative current values. The shape of these transients resembles the oscillating current transients mentioned above which are observed if reorientation of the adsorbed molecules during condensation takes place. The initial exponential decay of the current due to the charging of the double layer and dilute adsorption was in our case obviously so fast that with our instrumentation we were not able to observe it.

A different course shows the j–t curves obtained by stepping from $E_i = -0.2$ V (region Ib) to a different E_f in region II (E_f is located close to the positive edge of the capacitance pit), Fig. 6B. On the exponentially decaying part, there is a shoulder, at higher $|E_f - E_T|$ values, the shoulder appears sooner. The total current during the whole transition is negative, no oscillation current is observed. It can be thus supposed that during phase transitions from dilute adsorption region Ib to condensed region II, the reorientation of the adsorbed cytidine molecules does not occur.

Fig. 6C shows j–t curves for cytidine at pH 8.3 obtained by stepping from $E_i = -1.2$ V (region Ia) to a different E_f in

Table 1
Parameters of the curves (a)–(e) in Fig. 7A fitted according to Eq. (2)

E (V)	k_n ($\times 10^{-2}$ s^{-1})	k_g ($\times 10^{-4}$ s^{-2})
− 1.029	2.35	0.28
− 1.027	4.53	0.40
− 1.025	6.5	0.80
− 1.023	9.3	2.80
− 1.020	3.05	74.0

Table 2
Parameters of the curves (a)–(e) in Fig. 7B fitted according to Eq. (3)

E (V)	m	b ($\times 10^{-4}$ s^{-m})
− 0.3380	1.98	0.91
− 0.3393	1.99	1.44
− 0.3398	2.02	1.66
− 0.3410	2.08	2.33

Table 3
Parameters of the curves (a)–(e) in Fig. 7C fitted according to Eq. (3)

E (V)	m	b ($\times 10^{-6}$ s^{-m})
−0.3380	2.95	0.76
−0.3393	2.98	1.11
−0.3398	3.01	2.42
−0.3410	3.08	5.69

region II. The j–t curves at pH 8.3 looks very similar like those at pH 5.

3.4.2. C–t curves

The transitions Ia → II or Ib → II in acid and alkaline solution yield at low $|E_f - E_T|$ values a sigmoidal C–t transients (not shown) typical for a nucleation and growth process which used to be analysed by the Avrami equation [1,30–33].

Fig. 7 shows a plot of the degree of coverage of the condensed region vs. time (Θ–t) for interfacial transformations starting from the dilute adsorption region (states Ia or Ib) to the physisorbed film II in acid solution (Fig. 7A,B) and in alkaline solution (Fig. 7C). The degree of coverage Θ was calculated from the capacitance values as:

$$\Theta = (C_0 - C_t)/(C_0 - C_1) \quad (1)$$

where C_0 is the capacitance measured immediately after the potential step, and C_1 is the capacitance after the transient has reached a final steady state value.The experimental capacitance transients can be represented satisfactorily by the equation:

$$\Theta = 1 - \exp\Big(- k_g\big(t^2 - 2t/k_n + (2/(k_n)^2)(1 - \exp(-k_n t))\big)\Big) \quad (2)$$

in which k_g and k_n are growth and nucleation rate parameters, respectively [15]. For the two limiting cases of instantaneous nucleation ($k_n \to \infty$) and progressive nucleation ($k_n \to 0$), Eq. (2) simplifies to:

$$\Theta = 1 - \exp(-bt^m) \quad (3)$$

with $b = k_g$, $m = 2$ and $b = k_g k_n/3$, $m = 3$. The least-square fits of the measured transients over the whole time range were made using Eqs. (2) and (3) and working with nonlinear regression analysis.

Fig. 7A shows the theoretical fit experimentally measured Θ–t curves of Ia → II transient for different final potentials E_f at pH 5. It can be seen that the Θ–t curves are satisfactorily fitted by Eq. (2). Parameters of Θ–t curves fitted to Eq. (2) are given in Table 1.

Fig. 7B and C shows a comparison between the theoretically calculated and experimentally measured Θ–t curves of Ib → II transient at pH 5 and Ia → II transient at pH 8.3 for different E_f, respectively. Transients Ib → II for 30 mM cytidine are satisfactorily fitted by Eq. (3), namely instantaneous nucleation with $m = 2$ at pH 5. A progressive nucleation with $m = 3$ can be used for fitting of the rising part of the Ia → II transients at pH 8.3 (Fig. 7C). Parameters of Θ–t

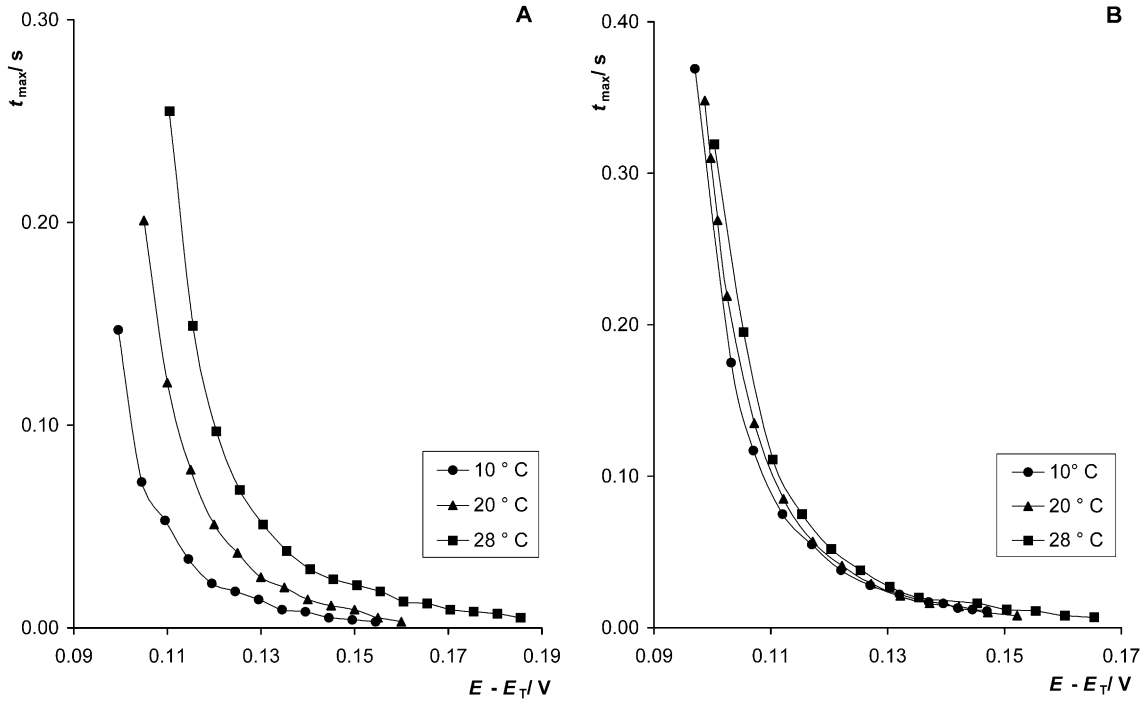

Fig. 8. The effect of temperature on the rate of the transformation of film Ia → II for 30 mM cytidine in 0.5 M NaCl + BR buffer at (A) pH 5 and (B) pH 8.3.

curves fitted to Eq. (3) are given in Table 2 (Ib → II transients at pH 5) and Table 3 (Ia → II transients at pH 8.3). At longer times, the decrease of Θ was observed, especially at pH 8.3, Fig. 7C. This might show that the ordered condensed film is not stable during the time and later starts to be destroyed. Such behaviour was observed earlier by Wandlowski and Pospisil [62,63] with an ordered film of uracil and by Vetterl and de Levie [21] with an ordered film of adenine.

3.4.3. Dependence of temperature, pH and ionic composition of the solution on the rate of transformations of cytidine films

Fig. 8A shows the effect of temperature and electrode potential on the rate of the transition Ia → II for 30 mM cytidine in 0.5 M NaCl + BR buffer at pH 5. The values on the horizontal axes are the differences between the final potential E_f and the true equilibrium transition potential E_T obtained from the $C–E–t$ plots (Fig. 2A). On the vertical axes, the t_{max} times at which the current reaches its maximum are plotted. Transition Ia → II is faster at higher values of $E - E_T$ and at lower temperatures. At higher $E - E_T$ values, temperature has almost no effect on the transformation rate. This is typical of a non-faradaic condensation process controlled by a nucleation and growth mechanism [33,64].

Fig. 8B shows the effect of temperature on the transformation Ia → II for 30 mM cytidine in 0.5 M NaCl + BR buffer at pH 8.3. It can be seen that temperature has almost no effect on the transformation rate. From $C–E–t$ surfaces (Fig. 3A), it can be concluded that during the establishment of interfacial equilibrium of condensed film of cytidine at potentials located close to the negative edge of capacitance pit (region II) at pH 8.3, a mixture of cytidine adlayers containing formed and/or dissolute nuclei centres coexists at the electrode surface. From theoretical fitting of the observed $C–t$ (Fig. 7C), it can be concluded that the transformation of the film Ia → II proceeds through a 2D progressive polynucleation and growth mechanism.

Transitions Ia → II are faster in acid solution than in alkaline or neutral solution. At higher values of $E - E_T$, the difference between the rate of transformation Ia → II in acid and alkaline solutions disappears.

Fig. 9 shows the effect of the ionic composition of the solution on the rate of transformation Ia → II for 30 mM cytidine, pH 5 at temperature 10 °C. In 0.5 M NaCl without BR buffer, there is almost linear dependence of the rate of transformation on E_f (Fig. 9). The rate of transformation depends exponentially on E_f both in 0.5 M BR buffer and in 0.5 M NaCl + BR buffer (Fig. 9). It can be seen that triggering of the phase transitions Ia → II needs higher activation energy both in 0.5 M BR buffer and in 0.5 M NaCl + BR buffer than in 0.5 M NaCl.

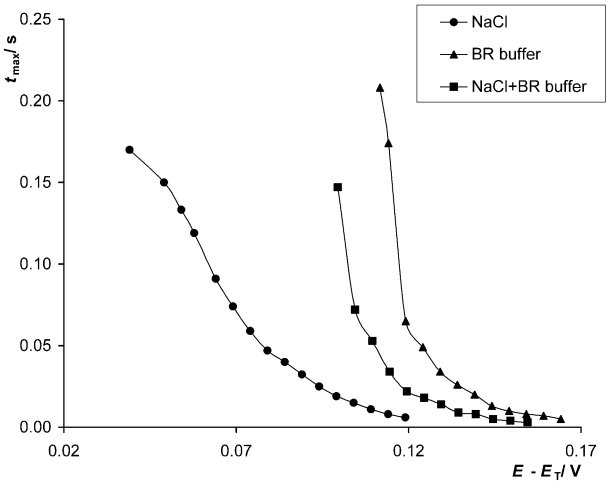

Fig. 9. The effect of the 0.5 M NaCl (●), 0.5 M BR buffer (▲) and 0.5 M NaCl + BR buffer (■) on the rate of transformation Ia → II for 30 mM cytidine, pH 5 at temperature 10 °C.

4. Conclusion

Depending on the potential applied to the electrodes, cytidine forms highly ordered two-dimensional adlayers, which were observed in a broad range of pH. In acid solvent, only one kind of condensed layer is formed. In alkaline solution, cytidine forms two different 2D adlayers. The centre of the first of them (region II) is located around − 0.8 V, the second 2D physisorbed film is formed at potentials more positive than − 0.3 V (region III). The extent of region III is only slightly affected by a temperature contrary to region II. From this behaviour of the region III, it can be assumed that at neutral and alkaline pH, cytidine is chemisorbed on HMDE. The driving forces stabilising the 2D condensed film of cytidine in region II seems to be stacking interaction.

In this paper, we have shown that the formation of a physisorbed film of cytidine molecules adsorbed at HMDE surface proceeds by a complex mechanism. From $C–E–t$ surfaces, it can be seen that the effect of time on the region II is more complicated in alkaline pH compared with acid pH.

From $j–t$ transients, it can be seen that during phase transformations from Ia to II, the reorientation of the cytidine molecules occurred at the HMDE surface both at pH 5 and pH 8.3. The transformations of the film Ia → II in acid and alkaline solution yield a sigmoidal $C–t$ transient. Experimentally measured $C–t$ transient were analysed by Avrami theorem. The rate of transformation of the interfacial states of cytidine is affected by the ionic composition and pH of the supporting electrolyte. The rate of the transformation depends on temperature at pH 5, but not at pH 8.3.

Acknowledgements

This work was supported by Grant Agency of the Ministry of Education, Youth and Physical Training of the

Czech Republic "Fund for Development of Universities" G4 0583 (S.H.) and F4 0564 (V.V.), Grant Agency of the Czech Republic, Grant No. 204/97/K084 and by the Grant Agency of the Academy of Sciences of the Czech Republic, Grant No. IAA 4004002 and S5004107.

References

[1] V. Brabec, V. Vetterl, O. Vrana, Electroanalysis of biomacromolecules, in: V. Brabec, D. Walz, G. Milazzo (Eds.), Experimental Techniques in Bioelectrochemistry, Birkhäuser Verlag, Basel, Switzerland, 1996, pp. 287–359.
[2] E. Palecek, From polarography of DNA to microanalysis with nucleic acid-modified electrodes, Electroanalysis 8 (1996) 7–14.
[3] E. Palecek, M. Fojta, DNA hybridization and damage, Anal. Chem. 73 (2001) 74A–83A.
[4] V. Vetterl, Alternating current polarography of nucleotides, J. Electroanal. Chem. 19 (1968) 169–173.
[5] Y.M. Temerk, P. Valenta, Electrochemical behaviour of mono- and oligonucleotides: Part V. Voltammetric studies on the adsorption stages and interfacial orientations of cytidine at charged interfaces, J. Electroanal. Chem. 93 (1978) 57–67.
[6] Y.M. Temerk, Studies on the adsorption and the association of cytidine sulphate at the dropping mercury electrode with phase-sensitive ac-polarography, Can. J. Chem. 57 (1979) 1136–1140.
[7] Y.M. Temerk, P. Valenta, H.W. Nürnberg, Electrochemical behaviour of mono- and oligonucleotides: Part VII. Comparative studies on the adsorption of cytidine at the mercury–aqueous solution interface by pulse polarography and ac polarography, J. Electroanal. Chem. 109 (1980) 289–300.
[8] V. Vetterl, J. Pokorný, Reorientation of the cytosine derivatives at the electrode surface, Bioelectrochem. Bioenerg. 7 (1980) 517–526.
[9] Y.M. Temerk, P. Valenta, H.W. Nürnberg, Electrochemical behaviour of mono- and oligonucleotides: Part 9. Voltammetric studies on the adsorption and association of the oligonucleotide cytidylyl-(3 → 5)-cytidine at the mercury–solution interface, J. Electroanal. Chem. 131 (1982) 265–277.
[10] M.M. Kamal, Z.M. Temerk, M.E. Ahmed, Z.A. Ahmed, The effect of pH on the adsorption and the association of cytidine, cytidine-5′-monophosphate and cytidine-5′-diphosphate at the charged interface, Bioelectrochem. Bioenerg. 16 (1986) 485–495.
[11] M.S. Ibrahim, Adsorption stages and interfacial orientations of cytidine sulfate at the mercury/electrolyte interface, Electrochim. Acta 40 (1995) 1913–1919.
[12] V. Vetterl, Adsorption of DNA components on the mercury electrode, Experientia 21 (1965) 9–11.
[13] V. Vetterl, Electric field effect in the adsorption of adenosine and cytosine, Bioelectrochem. Bioenerg. 3 (1976) 338–345.
[14] U. Retter, Two-dimensional nucleation in the adsorption of cytosine at the mercury–electrolyte interface, J. Electroanal. Chem. 106 (1980) 371–375.
[15] U. Retter, Two-dimensional one-step nucleation according to an exponential law in the formation of condensed adsorption films, J. Electroanal. Chem. 179 (1984) 25–29.
[16] J. Jursa, V. Vetterl, Effect of Cl^-, Br^- and I^- ions on the adsorption and association of cytosine at a mercury electrode, Bioelectrochem. Bioenerg. 12 (1984) 137–146.
[17] R. Sridharan, R. de Levie, Condensed thymine films at the mercury water interface: Part 5. Phase-transitions, J. Electroanal. Chem. 230 (1987) 241–256.
[18] U. Retter, V. Vetterl, J. Jursa, On the stability of condensed adsorption films, J. Electroanal. Chem. 274 (1989) 1–9.
[19] T. Wandlowski, On the time-dependence of the formation of condensed uracil films at the mercury electrolyte interface, Electroanal. Chem. 293 (1990) 219–236.
[20] H. Francois, M. Scharfe, C. Buess-Herman, A comparative study of the kinetics of formation of condensed monolayers of uracil and uridine at the mercury/water interface, J. Electroanal. Chem. 296 (1990) 415–428.
[21] V. Vetterl, R. de Levie, The effect of halide ions on the condensation of adenine at the mercury–water interface, J. Electroanal. Chem. 310 (1991) 305–315.
[22] T. Wandlowski, Some aspects of the kinetics of formation of condensed 5-methyluracil films at the mercury electrolyte interface, J. Electroanal. Chem. 333 (1992) 77–91.
[23] M. Scharfe, C. Buess-Herman, Multiple metastable states in the two-dimensional condensation of uridine at the mercury electrode, J. Electroanal. Chem. 366 (1994) 303–310.
[24] C. Prado, I. Navarro, M. Rueda, H. Francois, C. Buess-Herman, Kinetics of condensation of adenine at the mercury vertical bar electrolyte interface, J. Electroanal. Chem. 500 (2001) 356–364.
[25] C.M.A. Brett, A.M.O. Brett, Electrochemistry. Principles, Methods, and Applications, Oxford Univ. Press, Oxford, 1998.
[26] C. Mongay, V. Cerda, A Britton–Robinson buffer of known ionic strength, Ann. Chim. 64 (1974) 409–412.
[27] W. Lorenz, Über die Geschwindigkeit der adsorption und der zweidimensionalen assoziation höherer fettsäuren an der grenzfläche quecksilber-elektrolytlösung, Z. Elektrochem. 62 (1958) 192–200.
[28] I.R. Miller, The structure of DNA and RNA in the water–mercury interface, J. Mol. Biol. 3 (1961) 229–240.
[29] I.R. Miller, Temperature dependence of the adsorption of native DNA in a polarized water–mercury interface, J. Mol. Biol. 3 (1961) 357–361.
[30] C. Buess-Herman, Phase transitions in adsorbed layers, in: A.F. Silva (Ed.), Trends in Interfacial Electrochemistry and Electrochemical Engineering, NATO-ASI, Reidel, Dordrecht, 1986, pp. 205–253.
[31] R. de Levie, The dynamic double layer: two-dimensional condensation at the mercury–water interface, Chem. Rev. 88 (1988) 599–609.
[32] C. Buess-Herman, Dynamics of adsorption and two-dimensional phase transitions at electrode surfaces, in: J. Lipkowski, P.N. Ross (Eds.), Adsorption of Molecules at Metal Electrodes, VCH Publishers, New York, 1992, pp. 77–118.
[33] C. Buess-Herman, Self-assembled monolayers at electrode metal surfaces, Prog. Surf. Sci. 46 (1994) 335–375.
[34] J. Sponer, J. Leszczynski, V. Vetterl, P. Hobza, Base stacking and hydrogen bonding in protonated cytosine dimer: the role of molecular ion-dipole and induction interactions, J. Biomol. Struct. Dyn. 13 (1996) 695–706.
[35] M.H. Hölzle, T. Wandlowski, D. Kolb, Structural transitions in uracil adlayers on gold single-crystal electrodes, Surf. Sci. 335 (1995) 281–290.
[36] M.H. Hölzle, D.M. Kolb, D. Krznaric, B. Cosovic, Adsorption and phase formation of uracil derivatives on gold and silver single-crystal electrodes, Ber. Bunsen-Ges. 100 (1996) 1779–1790.
[37] S. Bare, C. Buess-Herman, On the formation and dissolution kinetics of two-dimensional uracil ordered phases at the gold single crystal electrode aqueous solution interface, Colloids Surf., A 134 (1998) 181–191.
[38] W.H. Li, W. Haiss, S. Floate, R.J. Nichols, In-situ infrared spectroscopic and scanning tunneling microscopy investigations of the chemisorption phases of uracil, thymine, and 3-methyl uracil on Au(111) electrodes, Langmuir 15 (1999) 4875–4883.
[39] S. Bare, M. Van Krieken, C. Buess-Herman, A. Hamelin, Effect of the crystallographic orientation of gold single-crystal electrodes on the occurrence of 2D phase transitions in adsorbed organic monolayers, J. Electroanal. Chem. 445 (1998) 7–11.
[40] M. Van Krieken, C. Buess-Herman, On the dissolution kinetics of two-dimensional uridine layers adsorbed on gold single-crystal electrodes, Electrochim. Acta 43 (1998) 2831–2841.
[41] M. Van Krieken, C. Buess-Herman, On the adsorption of uridine at the Ag(111)/aqueous solution interface, Electrochim. Acta 45 (1999) 675–683.

[42] T. Wandlowski, D. Lampner, S.M. Lindsay, Structure and stability of cytosine adlayers on Au(111): an in-situ STM study, J. Electroanal. Chem. 404 (1996) 215–226.
[43] K. Ataka, M. Osawa, In situ infrared study of cytosine adsorption on gold electrodes, J. Electroanal. Chem. 460 (1999) 188–196.
[44] N. Papadopoulos, C. Hasiotis, G. Kokkinidis, G. Papanastasiou, 3-Dimensional electrochemistry—utilization of $I–E–t$ curves for elucidation of electrochemical reactions, J. Electroanal. Chem. 308 (1991) 83–96.
[45] N. Papadopoulos, S. Sotiropoulos, P. Nikitas, 3-Dimensional phase-sensitive ac voltammetry for the study of adsorption processes—an application to the adsorption of sodium dodecyl-sulfate at the mercury electrolytic solution interface, J. Electroanal. Chem. 324 (1992) 375–385.
[46] F. David, H. Ouguenoune, A. Bolyos, N. Papadopoulos, Description of a 3-dimensional polarograph, Anal. Chim. Acta 292 (1994) 297–304.
[47] N. Papadopoulos, 3-Dimensional phase sensitive ac voltammetric study of the film development of phosphonium cations at a stationary mercury-electrode, Electrochim. Acta 37 (1992) 2447–2451.
[48] A. Avranas, N. Papadopoulos, Adsorption of surfactants—differential capacitance studies using phase-sensitive alternating-current voltammetry, Langmuir 8 (1992) 2804–2809.
[49] E. Bosco, S.K. Rangarajan, Electrochemical phase formation (ECPF)—nucleation growth vis-a-vis adsorption models, J. Electroanal. Chem. 129 (1981) 25–51.
[50] C. Buess-Herman, Non-faradaic phase transitions in adsorbed organic layers: Part 2. Experimental aspects, J. Electroanal. Chem. 186 (1985) 41–50.
[51] T. Wandlowski, Phase-transitions in uracil adlayers on Ag, Au, and Hg electrodes–substrate effects, J. Electroanal. Chem. 395 (1995) 83–89.
[52] C. Donner, S. Kirste, Influence of the electrolyte resistance on the transient response in nonfaradaic phase transition experiments on mercury and Au(111), Langmuir 17 (2001) 1630–1636.
[53] L. Pohlmann, C. Donner, H. Baumgartel, Predator–prey-like behaviour of the condensation process in two-dimensional adsorbate systems, J. Phys. Chem. B 101 (1997) 10198–10204.
[54] C. Donner, S. Kirste, L. Pohlmann, H. Baumgärtel, Inverted current–time transients. A new method for the determination of the potential of maximum adsorption in condensed layers, Langmuir 14 (1998) 6999–7007.
[55] C. Donner, L. Pohlmann, Interference of adsorption, condensation, and double-layer charging in kinetic studies of film formation: Part 1. Constant double-layer potential, Langmuir 15 (1999) 4898–4906.
[56] A. Bewick, M. Fleischmann, H.R. Thirsk, Kinetics of the electrocrystallization of thin films of calomel, Trans. Faraday Soc. 58 (1962) 2200–2216.
[57] M. Fleischmann, H.R. Thirsk, Metal deposition and electrocrystallization, in: P. Delahay, C. Tobias (Eds.), Advances in Electrochemistry and Electrochemical Engineering, Wiley-Interscience, New York, 1963, pp. 123–210.
[58] E. Bosco, S.K. Rangarajan, Some adsorption–nucleation-based models for electrochemical phase formation, J. Chem. Soc., Faraday Trans. 1, 77 (1981) 1673–1696.
[59] B. Bhattacharjee, S.K. Rangarajan, Adsorption nucleation growth based model for electrochemical phase formation and Avrami ansatz for a multicomponent competitive growth-process, J. Electroanal. Chem. 302 (1991) 207–218.
[60] M.H. Hölzle, U. Retter, D.M. Kolb, The kinetics of structural-changes in Cu adlayers on Au(111), J. Electroanal. Chem. 371 (1994) 101–109.
[61] C. Donner, L. Pohlmann, Interference of adsorption, condensation, and double-layer charging in kinetic studies of film formation: 2. Nonconstant double-layer potential, Langmuir 15 (1999) 4907–4915.
[62] T. Wandlowski, L. Pospisil, The growth of compact layers at the electrode interface: Part 2. The formation and stability of uracil films, J. Electroanal. Chem. 258 (1989) 179–192.
[63] T. Wandlowski, L. Pospisil, The growth of compact layers at the electrode interface: Part 4. Fractal character of uracil films at the mercury–aqueous electrolyte interface, J. Electroanal. Chem. 270 (1989) 319–329.
[64] C. Buess-Herman, S. Bare, M. Poelman, M. Van Krieken, Ordered organic adlayers at electrode surfaces, in: A. Wieckowski (Ed.), Interfacial Electrochemistry: Theory, Experiment and Applications, Marcel Dekker, New York, 1999, pp. 427–447.